

# Glucose Control Design Using Nonlinearity Assessment Techniques

**Nicholas Hernjak**

Dept. of Chemical Engineering, University of Delaware, Newark, DE 19716

**Francis J. Doyle III**

Dept. of Chemical Engineering, University of California, Santa Barbara, CA 93106

DOI 10.1002/aic.10326

Published online in Wiley InterScience (www.interscience.wiley.com).

*The most effective control algorithm for regulation of glucose levels in persons with diabetes is determined using control-relevant nonlinearity analysis of a diabetic system model. Theoretical control-relevant nonlinearity analysis is performed using the Optimal Control Structure and a norm-based nonlinearity measure. These results are correlated with results of controller performance assessment trials, based on optimizing the rejection of glucose disturbances. Performance is quantified using a standard quadratic performance objective as well as an asymmetric performance objective in which negative glucose deviations are penalized more highly than positive deviations because of the greater health concerns associated with negative deviations. The control-relevant nonlinearity assessment indicates that the best controller design is a linear algorithm except when the desired performance is strongly asymmetric. For standard meal disturbances, the system is found to be well regulated using proportional-derivative control or standard linear model predictive control with no significant benefit observed in using nonlinear model-based control. © 2005 American Institute of Chemical Engineers AICHE J, 51: 544–554, 2005*

*Keywords: diabetes, nonlinearity characterization, nonlinear control, optimal control, performance assessment*

## Introduction

The lifestyles of those living with diabetes are often severely affected by the consequences of the disease. Because of the inability of the pancreas to regulate blood glucose levels, patients typically regulate glucose manually. This task often involves the patient extracting blood samples to use in measuring glucose levels. Based on the obtained glucose measurements, patients must then decide whether boluses of insulin beyond those of their daily regimen are required. For inexperienced or less-conscientious patients, the glucose regulation

task can be easily mishandled, potentially leading to a number of health problems including heart and blood vessel disease, kidney disease, blindness, and comas, the consequence of which may be a shortened life span.<sup>1</sup> Deviations below the basal glucose levels (hypoglycemic deviations) are considerably more dangerous in the short term than positive (hyperglycemic) deviations, although both types of deviations are undesirable.

Realizing the inherently problematic nature of self-regulation of glucose, systems researchers have actively pursued automated regulation systems. Physicians also recognize the benefits of automated techniques and are beginning to address the physiologically relevant issues that need to be considered before such techniques become realities (for example, Wolpert<sup>2</sup>). A closed-loop glucose regulation system requires three

Correspondence concerning this article should be addressed to F. J. Doyle III at [doyle@engineering.ucsb.edu](mailto:doyle@engineering.ucsb.edu).

components: a glucose sensor, an insulin-delivery device, and a control algorithm. Beginning with the measurement issue, sensors have been developed that provide glucose readings as frequently as every 10 min, thus making automated regulation a realizable possibility. Examples of these devices include the *MiniMed*® CGMS® device<sup>3</sup> and the noninvasive *Glucowatch*®.<sup>4</sup> The automated insulin delivery device is realized as a computer-controlled pump that delivers insulin amounts based on the readings from the glucose sensor. The commonly available pumps (such as those by *Disetronic*<sup>5</sup> and *MiniMed*®<sup>6</sup>) are externally worn and allow the user to enter insulin bolus amounts on-demand or to preprogram bolus amounts and times. For control, researchers have investigated a wide range of algorithms, including simple proportional–integrative–derivative (PID) algorithms<sup>7,8</sup> as well as linear<sup>9</sup> and nonlinear<sup>10</sup> model predictive control (MPC) algorithms. Also, a number of researchers have investigated nonlinear optimal control techniques (see, for example, Ollerton<sup>11</sup> and Fisher<sup>12</sup>).

The researchers that have investigated nonlinear control techniques recognize the inherent nonlinearity of the diabetic system. The assumption implied in their work is that the system nonlinearity is significant enough over the typical operating range that nonlinear control is required to optimally regulate the system. Likewise, the proponents of linear control techniques assume that the nonlinearity of the system is not severe enough to warrant nonlinear control and rely on the inherent robustness of, say, linear MPC schemes to compensate for the mismatch between the incorporated linear model and the system itself.

The objective of this work is to determine the optimal control algorithm for glucose regulation based on an assessment of the control-relevant nonlinearity of a diabetic system model. The technique involves use of a numerical nonlinearity measure to quantify the severity of the nonlinearity of a control-relevant system. By quantifying the control-relevant nonlinearity, the necessary degree of controller nonlinearity is determined. It is assumed that a system with low control-relevant nonlinearity will be controlled optimally using linear techniques with no additional benefit in using nonlinear techniques. Conversely, a system with high control-relevant nonlinearity will be controlled optimally only through use of nonlinear techniques. Control-relevant nonlinearity is a function of the inherent system nonlinearity, the operating region, and the system performance objective.

Regarding the performance objective of the diabetic system, the typical and, perhaps, most immediately intuitive choice is minimization of integral-squared glucose deviation from the basal level. A performance objective including this factor is considered first in the analysis. As mentioned previously, it is known that negative glucose deviations are more dangerous than positive glucose deviations. Therefore, consideration is also given to an asymmetric performance objective in which negative deviations are penalized more than positive deviations.<sup>13</sup>

In the next section, an overview of control-relevant nonlinearity characterization theory and methodology is provided. The diabetic system model that is considered in this work is then described and a preliminary assessment of its open-loop properties performed. Assessment of control-relevant nonlinearity is then performed for the standard and asymmetric objective functions and a set of controllers is assessed for perfor-

mance and the results compared to those of the nonlinearity assessment. The results are then summarized and the work is concluded with recommendations based on the analysis.

## Control-Relevant Nonlinearity Characterization

Assessment of control-relevant nonlinearity is a critical step in the design of control structures for nonlinear systems. As the authors have shown previously,<sup>14</sup> it is generally insufficient to assess only the open-loop nonlinearity of a system because the desired controller performance plays a strong role in determining the aspects of the open-loop nonlinearity that are relevant to the closed loop. Also, achieving a complex performance objective may result in nonlinear effects beyond those of the open-loop process.

Assessment of control-relevant nonlinearity requires two components: a numerical measure of nonlinearity and a control-relevant system to be characterized. These items are considered, respectively, in the next two subsections.

### Nonlinearity measure

The concept of a measure of nonlinearity was first proposed by Desoer and Wang<sup>15</sup> in demonstrating the linearizing effects of linear feedback. Haber<sup>16</sup> was the first to propose a series of practical, data-driven nonlinearity tests used primarily to detect the presence of nonlinearity, as opposed to quantifying nonlinearity severity. Researchers have continued to develop nonlinearity measures based on various quantification principles, including: differences in steady-state gain over an operating region,<sup>17</sup> measures of steady-state map curvature,<sup>18</sup> norm-based quantification using a novel inner product definition,<sup>19</sup> and comparison of empirical and theoretical gramians.<sup>20</sup>

For this work, the nonlinearity measure proposed by Allgöwer<sup>21</sup> is used to quantify nonlinear severity. This measure is directly based on the work of Desoer and Wang.<sup>15</sup> The nominal form of the measure is given as

$$\phi_N^{\mathcal{U}} = \inf_{G \in \mathcal{G}} \sup_{u \in \mathcal{U}} \frac{\|G[u] - N[u]\|_{p\mathcal{Y}}}{\|N[u]\|_{p\mathcal{Y}}} \quad (1)$$

where  $\mathcal{U}$  is the space of admissible input signals,  $N: \mathcal{U} \rightarrow \mathcal{Y}$  is the system operator,  $G: \mathcal{U} \rightarrow \mathcal{Y}$  is a linear approximation to  $N$ , and  $\mathcal{G}$  is the space of linear operators. The norm  $\|\cdot\|_{p\mathcal{Y}}$  denotes a  $p$ -norm defined on the space of output signals,  $\mathcal{Y}$ . Any admissible norm may be used in computing the measure, but it is prudent to consider a norm that has relevance for the problem under consideration. By definition,  $\phi_N^{\mathcal{U}}$  characterizes nonlinearity based on the best linear approximation given the “worst” input signal.

The nonlinearity measure  $\phi_N^{\mathcal{U}}$  will yield results in the range  $[0, 1]$ , where a value of 0 indicates a linear process (across the set of inputs considered) and values approaching 1 indicate a severely nonlinear process. Nominally,  $\phi_N^{\mathcal{U}}$  is well defined only for bounded-input, bounded-output (BIBO) stable systems. Helbig et al.<sup>22</sup> extended the measure definition to consider transient systems by allowing for minimization of the measure over the set of initial conditions and by limiting the possible definitions of  $\|\cdot\|_{p\mathcal{Y}}$  to finite-time norms.

As defined in Eq. 1, the computation of  $\phi_N^{\mathcal{U}}$  involves the solution of an infinite-dimensional min–max problem and is,

therefore, infeasible. To simplify the problem, the space  $\mathcal{U}$  may be limited to a representative set  $\mathcal{U}_c \subset \mathcal{U}$ . Next, a restricted version of  $\mathcal{G}$  is realized through use of a parameterized linear approximation (such as for a SISO system), as follows

$$G[u(s)] = w_o u(s) + \sum_{i=1}^{N_l} \frac{w_i}{\tau_i s + 1} u(s) \quad (2)$$

To compute the nonlinearity measure, one selects the number of basis functions ( $N_l$ ) and the corresponding set of time constants ( $\tau_i$ ) and then performs a minimization to find the optimal set of weights ( $w_i$ ) for the  $u \in \mathcal{U}_c$  that maximizes the measure. It has been shown that the search for the optimal weight set is convex.<sup>21</sup> Given the above restrictions, the nonlinearity measure approximation can be written as

$$\phi_N^u \approx \min_{w \in \mathbb{R}^{N_l+1}} \max_{u \in \mathcal{U}_c} \frac{\|G[u] - N[u]\|_{P^2y}}{\|N[u]\|_{P^2y}} \quad (3)$$

where  $G[u]$  is represented by Eq. 2.

### Optimal control structure

Control-relevant nonlinearity will be characterized through use of the optimal control structure (OCS). Stack and Doyle<sup>23</sup> proposed the OCS as a control-relevant system that incorporates the three components of control-relevant nonlinearity: the open-loop system, operating region, and performance objective.

The OCS is a relaxation of the solution to the classical optimal control problem. Given a process model  $[x(t) \in \mathbb{R}^n, u(t) \in \mathbb{R}^m]$ :

$$\dot{x} = f(x, u) \quad x(0) = x_o \quad (4)$$

and a performance objective (without endpoint penalty)

$$\mathcal{J}[u(t)] = \int_0^{t_f} F(x, u) dt \quad (5)$$

the Hamiltonian,  $\mathcal{H}$ , is defined as follows, where  $\lambda(t) \in \mathbb{R}^n$  are the system costates

$$\mathcal{H} = F(x, u) + \lambda^T f(x, u) \quad (6)$$

The OCS is composed of two of the three sets of necessary conditions that define the solution to the classical optimal control problem, that is

$$\frac{\partial \mathcal{H}}{\partial u} = 0 \quad (7)$$

$$\frac{\partial \mathcal{H}}{\partial x} = -\dot{\lambda}^T \quad \lambda(t_f) = 0 \quad (8)$$

The third necessary condition in the classical optimal control law computation that is omitted in OCS analysis is

$$\frac{\partial \mathcal{H}}{\partial \lambda} = \dot{x} \quad x(0) = x_o \quad (9)$$

By inspection of the form of the Hamiltonian, it is obvious that Eq. 9 reduces to Eq. 4. Therefore, by ignoring the third condition, it is implied that the solutions to the OCS will *not* satisfy the open-loop process model. This approximation is introduced only to simplify the analysis because it allows one to avoid solving the two-point boundary value problem that arises in the traditional optimal control calculation.

The standard methodology for characterization of the OCS is to treat Eqs. 7 and 8 as a relaxed inverse of the open-loop model. To perform nonlinearity characterization, one selects a relevant set of  $x(t)$  (OCS inputs) and solves the OCS to obtain  $u(t)$  (OCS outputs). These signals can then be used to compute the nonlinearity measure (Eq. 1) for the OCS. If one lacks the system knowledge necessary to determine a relevant set of states to use for analysis, an appropriately broad set of generic state trajectories could be used (such as stochastic signals).

A typical procedure for use of the OCS is as follows. First, note that the OCS equations represent a pair of algebraic and differential equations

$$\Omega_1(\lambda, x, u) = 0 \quad (10)$$

$$\Omega_2(\lambda, x, u) = \dot{\lambda} \quad \lambda(t_f) = 0 \quad (11)$$

By the implicit function theorem, Eq. 10 will, at least, implicitly define an expression for the OCS output,  $u(t)$ , as a function of  $x(t)$  and  $\lambda(t)$  in the neighborhood of a point  $(\lambda_o, x_o, u_o)$  [such that  $\Omega_1(\lambda_o, x_o, u_o) = 0$ ] provided that the Jacobian of  $\Omega_1$  with respect to  $u$  is nonsingular. If this function can be explicitly derived, the OCS output can then be expressed by a new function,  $\omega(\cdot)$

$$u(t) = \omega[\lambda(t), x(t)] \quad (12)$$

Before continuing, note that the condition that the Jacobian of  $\Omega_1$  be nonsingular implies the following

$$\left| \frac{\partial^2 \mathcal{H}}{\partial u^2} \right|_{(\lambda_o, x_o, u_o)} \neq 0 \quad (13)$$

This condition signifies that the implicit function theorem will be valid provided that the value of the system's Hamiltonian is not at an inflection or saddle point with respect to  $u(t)$ .

Using Eq. 12, the expression defining the system costates can then be written as

$$\dot{\lambda} = \Omega_2[\lambda, x, \omega(\lambda, x)] \quad \lambda(t_f) = 0 \quad (14)$$

$$= \Omega_3(\lambda, x) \quad \lambda(t_f) = 0 \quad (15)$$

If all of the above conditions hold, the OCS can be visualized as shown in Figure 1. In integrating the OCS, the end-point

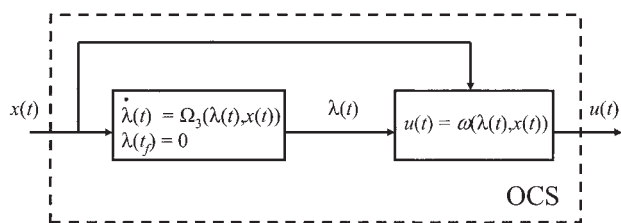


**Figure 1. Structural form of the OCS for special cases.**

condition on  $\lambda(t)$  can be handled by integrating  $\Omega_3$  in reverse time.

## System Model and Open-Loop Characterization

Several detailed models of diabetic systems exist in the literature including, for example, the 21st-order metabolic model of Sorensen.<sup>24</sup> To have a system that can be readily analyzed using the OCS techniques, this work focuses on the three-state minimal patient model of Bergman<sup>25</sup>

$$\begin{aligned}\dot{G} &= -p_1 G - X(G + G_B) + P(t) \\ \dot{X} &= -p_2 X + p_3 I \\ \dot{I} &= -n(I + I_B) + u(t)/V_I\end{aligned}\quad (16)$$

Note that the system states are in terms of deviation variables. Table 1 includes the definition of the three states (with initial conditions) and the model parameters for a nondiabetic individual. The control problem for this system is to maintain the glucose level,  $G(t)$ , near the basal condition using the exogenous insulin infusion rate,  $u(t)$ , given glucose disturbances entering as  $P(t)$ . Although this model is low order, it has been shown to demonstrate the essential dynamics of the glucose regulation system.

To alter the model to reflect a system with diabetes, the value for  $p_1$  is significantly reduced, often, for theoretical purposes, taking the value to be 0.<sup>26</sup> To consider the properties of the model and to consider the effects of reducing  $p_1$ , first consider the model linearization. Inspection of the system of relationships in Eq. 16 shows that the only nonlinear structure in the model is the bilinear term in the state equation describing  $G(t)$  evolution. Therefore, the system linearization is given as [for  $P(t) = 0$ ]

$$G(s) = \frac{-\frac{p_3}{V_I}(G_o + G_B)}{[s + (p_1 + X_o)](s + p_2)(s + n)} u(s) \quad (17)$$

where  $G_o$  and  $X_o$  are the initial conditions for glucose and remote compartment insulin utilization, respectively. For initial conditions in which plasma insulin is at its basal level (that is,  $I_o = 0$ ), remote compartment insulin utilization will also be 0, and thus, typically,  $X_o = 0$ . Inspection of Eq. 17 shows that, given  $X_o = 0$ , as  $p_1 \rightarrow 0$ , one of the system poles will tend toward zero, thus giving the model integrating action in the limit.

The behavior of the model is demonstrated by considering responses to a +20 mg/dL change in glucose initial conditions for various values of  $p_1$ , as shown in Figure 2. The responses

show that for values of  $p_1 > 0$ , the perturbed glucose level will return to basal conditions but at increasingly slow rates for decreasing values of  $p_1$ . For the limiting case of  $p_1 = 0$ , the system is unable to regulate the glucose level on its own. Based on these observations, this work will consistently analyze the system model with  $p_1 = 0$  because this represents a worst-case scenario in terms of difficulty of the system dynamics for control purposes.

To provide a basis of comparison for the control-relevant nonlinearity characterization results in the next section, the nonlinearity of the open-loop system model with  $p_1 = 0$  is considered. A set of 54 positive and negative insulin pulses is selected. A representative set of these inputs along with the resulting outputs are shown in Figure 3. Negative (deviation) pulses are admissible because the model receives a constant insulin input of 16.7 mU/min at steady state [chosen so that  $I(t) = 0$  at steady state]. Therefore, any negative deviation that does not surpass -16.7 mU/min is realizable. Throughout this work, the range of glucose excursions investigated will be approximately  $\pm 40$  mg/dL. Therefore, the inputs are selected such that the resulting glucose levels remain within the desired range. Note that, as will be used throughout this work, the length of time investigated is 360 min (6 h).

For the parameterized linear system (Eq. 2) used in computing the nonlinearity measure, 20 first-order basis functions are chosen with time constants logarithmically spaced between 25 and 600 min. Also, a direct feed-through term and a pure integrator are included. A standard, finite-time 2-norm was used in the computation of the nonlinearity measure as 2-norms will be used later to assess controller performance. Given the above conditions, the nonlinearity of the open-loop system is measured as 0.15. This result is quite low, thus indicating that the magnitude of the open-loop nonlinearity is mild in the operating range considered.

## Determination of the Optimal Control Algorithm

The relevant performance criterion for this system involves minimization of glucose deviation from the basal level. The specific objective that will be investigated has the following form

**Table 1. Parameter and Initial Condition Values for the System Model (16) for a Healthy Individual of Average Weight\***

Symbol	State/Parameters	Value
$G(t)$	Plasma glucose deviation	0 mg/dL
$X(t)$	Remote compartment insulin utilization	0 min <sup>-1</sup>
$I(t)$	Plasma insulin deviation	0 mU/dL
$G_B$	Basal glucose level	110 mg/dL
$I_B$	Basal insulin level	1.5 mU/dL
$p_1$	Model parameter	0.028 min <sup>-1</sup>
$p_2$	Model parameter	0.025 min <sup>-1</sup>
$p_3$	Model parameter	0.00013 dL/mU · min <sup>2</sup>
$n$	Model parameter	5/54 min <sup>-1</sup>
$V_I$	Insulin distribution volume	120 dL
$P(t)$	Exogenous glucose infusion rate	0 mg/dL · min
$u(t)$	Exogenous insulin infusion rate	16.7 mU/min

\*From Furler et al.<sup>26</sup>

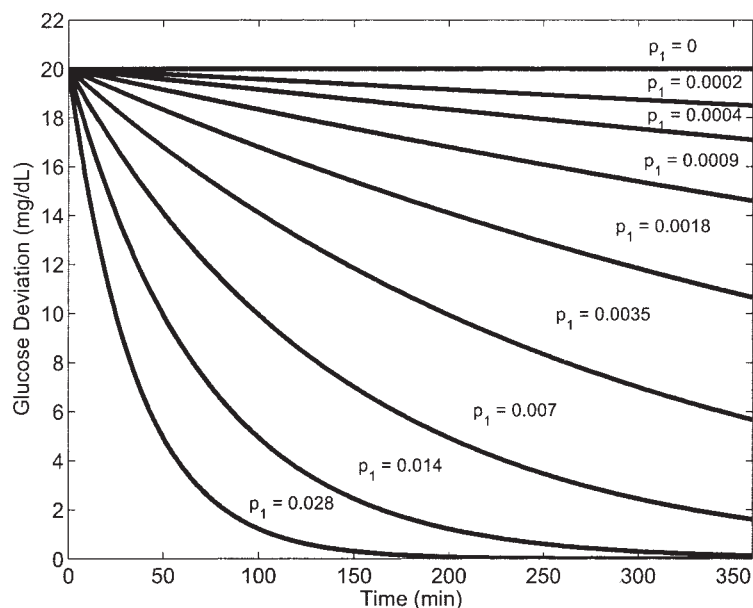


Figure 2. Response of the system model to a +20 mg/dL change in glucose initial conditions for varying values of  $p_1$ .

$$\mathcal{J}_p[u(t)] = \int_0^{t_f} \frac{1}{2} \{ \Gamma_y [\max(G(t), 0)^2 + \alpha \min(G(t), 0)^2] + \Gamma_u u^2(t) \} dt \quad (18)$$

where  $\alpha$  is the asymmetric performance weight,  $\Gamma_y$  is the error weight, and  $\Gamma_u$  is the move suppression weight. When  $\alpha = 1$ , Eq. 18 reduces to the standard quadratic performance objective. Results will be shown for varying values of  $\alpha$  corresponding to

variation of the magnitude of importance placed on minimizing hypoglycemic deviations over hyperglycemic deviations.

In this section, control-relevant nonlinearity is assessed using two methods. In the next subsection, the system's OCS nonlinearity is characterized to assess the theoretical control-relevant nonlinearity. The performance of a spectrum of controllers of varying algorithmic complexity is then assessed in meal disturbance rejection trials. The controllers include linear and nonlinear algorithms. Correlations are then sought between the theoretical assessment and the performance-based assessment with the assumption being that a system with high control-relevant nonlinearity will require highly nonlinear control to optimally regulate the system.

### OCS characterization

To derive the system OCS given the inherently discontinuous objective function (Eq. 18), the function  $\Xi(\cdot)$  is first defined

$$\Xi[G(t)] = \begin{cases} \frac{1}{2} G^2(t) & G(t) \geq 0 \\ \frac{1}{2} \alpha G^2(t) & G(t) < 0 \end{cases} \quad (19)$$

The derivative of  $\Xi$  with respect to  $G$  is given as

$$\frac{\partial \Xi}{\partial G} = \begin{cases} G(t) & G(t) \geq 0 \\ \alpha G(t) & G(t) < 0 \end{cases} \quad (20)$$

The system OCS is then expressed as

$$\dot{\lambda}_1 = -\Gamma_y \frac{\partial \Xi}{\partial G} + \lambda_1 X$$

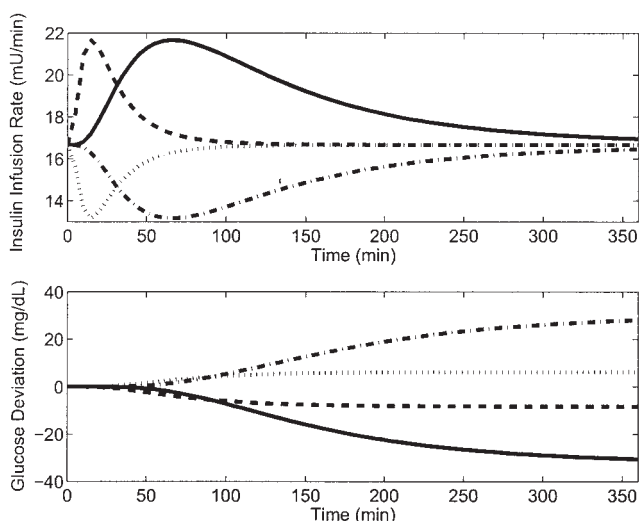
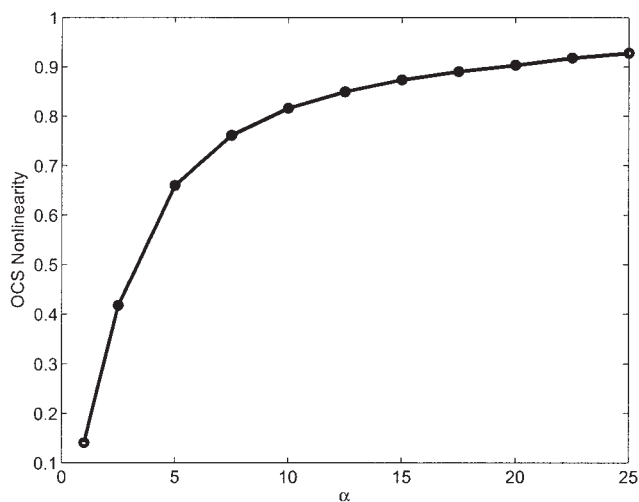


Figure 3. Representative inputs (top) and the resulting outputs (bottom) used in the open-loop diabetic system nonlinearity characterization.

Insulin delivery amounts: solid = positive delivery of 719 mU; dashed = positive delivery of 168 mU; dotted = negative delivery of 118 mU; dash-dotted = negative delivery of 503 mU.





**Figure 4. OCS nonlinearity as a function of the asymmetric performance weight  $\alpha$ .**

$$\begin{aligned}
 \dot{\lambda}_2 &= \lambda_1(G + G_B) + p_2\lambda_2 \\
 \dot{\lambda}_3 &= -p_3\lambda_2 + n\lambda_3 \\
 \lambda(t_f) &= 0 \\
 u(t) &= -\frac{\lambda_3}{2\Gamma_u V_I} \quad (21)
 \end{aligned}$$

In performing nonlinearity analysis of the OCS, the relevant input is  $G(t)$ , given that this is the only state affected by a glucose disturbance. Therefore, for this analysis,  $X(t) = 0$ .

As inputs to the OCS, integrated pulses are provided through  $G(t)$ . Integrated pulses are chosen because the disturbances entering the open-loop model through  $P(t)$  correspond to meals and are, therefore, nonpersistent. The effect of a pulse in  $P(t)$  on  $G(t)$  is approximately an integrated version of the pulse for  $p_1 = 0$ . For this analysis, the pulse magnitudes were chosen such that the integrated signals span the desired range of  $G(t)$ .

Beginning with  $\alpha = 1$ , OCS nonlinearity characterization is performed for various values of  $\Gamma_u$  ( $\Gamma_y$  will always be taken to be 1). The results are found to be insensitive to  $\Gamma_u$  and the resulting OCS nonlinearity is 0.14 over the inputs considered. Similar to the open-loop characterization result of 0.15, this result indicates mild nonlinearity. It can then be stated that the control-relevant nonlinearity at  $\alpha = 1$  is low, indicating that low-complexity, linear control techniques should optimally regulate the system.

Next, the OCS nonlinearity is characterized as a function of increasing  $\alpha$ . Using the same set of positive and negative input signals, the results in Figure 4 are obtained. The results show that the magnitude of the nonlinearity measure rises sharply with increasing  $\alpha$  and begins an asymptotic approach toward the maximum value of 1. These results indicate that as a greater preference is placed on reducing negative deviations, the nonlinearity of the necessary controller rises significantly.

### Performance assessment

To verify the conclusions drawn in the previous subsection, performance assessment trials are considered next for a set of controllers of varying complexity designed for the diabetic

system model (Eq. 16). The controllers investigated include standard proportional control (denoted as P-only), standard proportional-derivative (PD) control, and linear and nonlinear model predictive control (MPC and NMPC, respectively). The controllers are implemented in discrete formulations with sampling times of 5 min. The discrete formulation of the PD controller is

$$u(k) = K_c\{e(k) + K_d[e(k) - e(k-1)]\} \quad (22)$$

where  $k$  represents the  $k$ th time step,  $K_c$  is the proportional gain,  $e(k)$  is the set-point error at time  $k$ , and  $K_d$  is the derivative gain. P-only control is realized by setting  $K_d = 0$ . Note that there is no need to consider a controller with explicit integral action (such as PID) because the effect of setting  $p_1 = 0$  places an integral component in the closed-loop system and will thus eliminate steady-state offset.

The MPC algorithms are realized by including the exact state-space system model (Eq. 16) in the NMPC algorithm and the same model in the linear MPC but with the state equation for  $G(t)$  replaced with a linearized approximation as follows

$$\begin{aligned}
 \dot{G} &= -p_1G - XG - XG_B + P \\
 \dot{G} &\approx -p_1G - X_oG_o - X_oG - G_oX - XG_B + P \quad (23)
 \end{aligned}$$

where  $X_o$  and  $G_o$  represent initial conditions on remote compartment insulin utilization and plasma glucose. The following performance objective is used in the algorithms (note the similarity to Eq. 18)

$$\begin{aligned}
 \mathcal{J}_C[u(k)] &= \sum_{i=1}^p \Gamma_{yc}[\max(\hat{G}(k+i|k), 0)^2 \\
 &\quad + \alpha_c \min(\hat{G}(k+i|k), 0)^2] + \Gamma_{uc}u(k+i-1)^2 \quad (24)
 \end{aligned}$$

where  $\hat{G}(k+i|k)$  denotes the predicted value of plasma glucose at time step  $k+i$  given information up to the current time  $k$ .  $\Gamma_{yc}$ ,  $\Gamma_{uc}$ , and  $\alpha_c$  are the controller performance weights and are defined similarly to the corresponding weights in Eq. 18.  $p$  is the length of the prediction horizon and  $c$  is the length of the move horizon over which values of  $u(k)$  are varied. For  $k+c \leq t \leq k+p$ ,  $u(k)$  is held constant. Along with the performance weights,  $p$  and  $c$  are two critical tuning parameters in the MPC algorithms [for an overview of MPC algorithms, see Prett and Garcia (linear MPC)<sup>27</sup> and Allgöwer et al. (NMPC)<sup>28</sup>]. Similar to what one often observes in the tuning of PID-type controllers, variation of the MPC tuning parameters can result in significant qualitative changes in the system responses. For example, increasing the aggressiveness of the closed-loop responses through reduction of the value of  $\Gamma_{uc}$  may introduce oscillatory character in the system trajectories. In the results that will be shown, only quantitative information is used to determine controller tunings without regard to the resulting qualitative character of the responses.

The MPC optimizations are performed using Matlab's *fminunc* unconstrained optimization solver and a sequential programming technique. Although sequential techniques tend to be impractically slow, the small size of this problem allowed

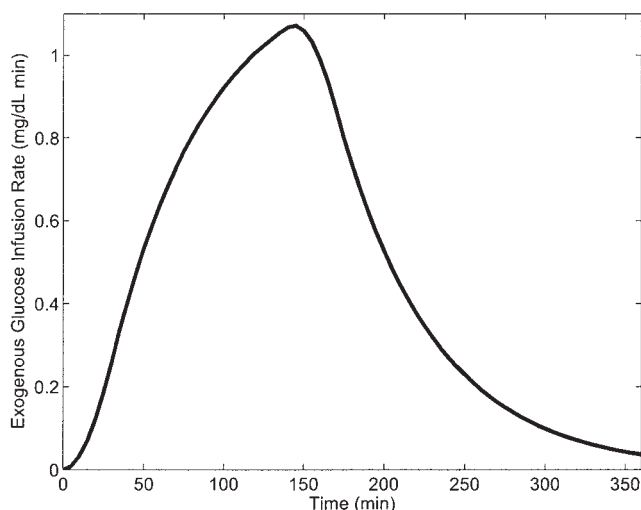


**Figure 5. Exogenous glucose infusion trajectory  $[P(t)]$  in Eq. 16] used to assess controller performance.**

the computations to be done within 10 s per time step on a PC with a *Pentium 4* 2.4-GHz processor with 512 MB RAM. Full state feedback without an explicit state estimator is assumed to avoid the additional degrees of freedom in estimator design.

Although an unconstrained optimization solver is used in computing the MPC outputs, note that the glucose control problem does have a physically meaningful constraint on the insulin input. That is, the insulin input cannot be less than zero ( $-16.7$  mU/min in terms of the deviation variables used in this work). Initially, this constraint will be satisfied through clipping of the controller outputs. In the final control trials, the effect of including more sophisticated constraint handling in the MPC algorithms is investigated.

The performance of the algorithms is assessed over a period of 6 h given meal disturbances modeled using the approach of Lehmann and Deutsch.<sup>29</sup> Using this approach, it is assumed that the rate of absorption of glucose through the gut wall can be modeled by a static linear relationship, that is,

$$R_{abs} = K_{abs} G_{gut} \quad (25)$$

where  $R_{abs}$  is the rate of absorption (mg/min),  $G_{gut}$  is the concentration of glucose in the gut (mg/dL), and  $K_{abs}$  is a constant taken to be  $0.0167 \text{ min}^{-1}$ . The material balance for glucose concentration in the gut is then given as

$$\dot{G}_{gut} = R_{emp} - K_{abs} G_{gut} \quad (26)$$

where  $R_{emp}$  is the rate of gastric emptying (mg/min) and is often taken to be a trapezoidal function representing the meal. By integrating  $R_{emp}$  as a function of time, the size of the meal is quantified. To calculate  $P(t)$ ,  $R_{abs}$  is simply scaled by the glucose distribution volume  $V_G$  (117.0 dL) to determine the glucose infusion rate per volume.

For the first trial, controller performance is assessed for a 20-g meal modeled using the meal disturbance model described above. The resulting form of  $P(t)$  is shown in Figure 5. The controller objective is to minimize the symmetric performance objective (Eq. 18) with  $\alpha = 1$  (that is, a quadratic performance

**Table 2. Controller Tunings and Performance Objective Values for Trials with  $\alpha = 1$ ,  $\Gamma_y = 1$ , and  $\Gamma_u = 1$  in Eq. (18)**

Controller	Tunings	Objective Value
P-only	$K_c = -0.29$	$4.73 \times 10^5$
PD	$K_c = -0.24$ , $K_d = 24.8$	$2.61 \times 10^5$
MPC	$p = 70$ , $c = 5$ , $\Gamma_{uc} = 0.01$ , $\Gamma_{yc} = 1.0$	$1.78 \times 10^5$
NMPC	$p = 70$ , $c = 5$ , $\Gamma_{uc} = 0.01$ , $\Gamma_{yc} = 1.0$	$1.61 \times 10^5$

objective),  $\Gamma_y = \Gamma_u = 1$ , and  $t_f = 360$  min. Each controller was tuned independently to find the minimum obtainable value for Eq. 18 for the particular algorithm. For this trial, the MPC algorithms with asymmetric objective functions ( $\alpha_c \neq 1$ ) are not considered because the considered disturbance will not yield significantly negative glucose deviations.

For the first trial, the determined tunings are given in Table 2 along with the resulting values of the performance objective. For the P-only and PD algorithms, the reported tunings correspond to tunings that yield an absolute minimum for the performance objective value. For the MPC and NMPC algorithms, it is found that, for fixed values of  $p$  and  $c$ , the resulting performance objective values for these algorithms asymptotically approach a minimum value with decreasing  $\Gamma_{uc}$ , as shown in Figure 6. Figure 7 compares the MPC and NMPC trajectories for several values of  $\Gamma_{uc}$  with  $p = 70$  and  $c = 5$  because these values are found to be the optimal choices for the horizon lengths. It is seen that for decreasing values of  $\Gamma_{uc}$ , the controller response is quicker but at a cost of decreased decay ratio. For longer trial lengths, the oscillations are seen to persist. Based on the results in Figures 6 and 7, the tuning of  $\Gamma_{uc} = 0.01$  found in Table 2 is selected as an acceptable value.

The input and output trajectories for the four controllers given the tunings listed in Table 2 can be found together in Figure 8. The results indicate that purely proportional control is the least acceptable option of the controllers investigated in

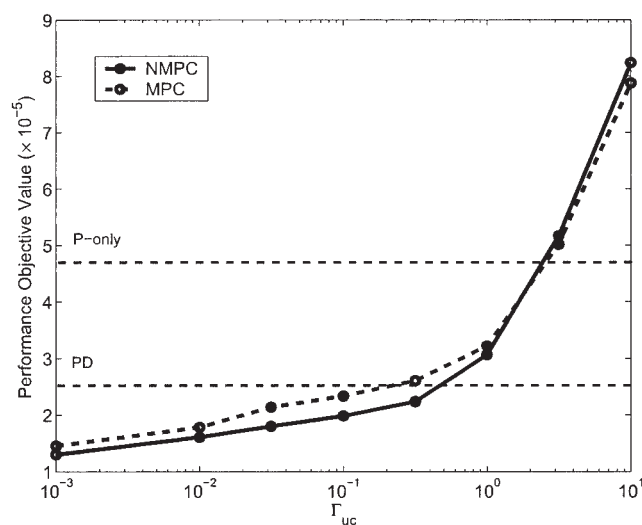


**Figure 6. Performance objective (Eq. 18) value as a function of  $\Gamma_{uc}$  for the MPC and NMPC algorithms with  $p = 70$ ,  $c = 5$ ,  $\Gamma_{yc} = 1$ , and  $\alpha_c = 1$ .**

The P-only and PD optimal performance results are shown as dotted lines for reference.

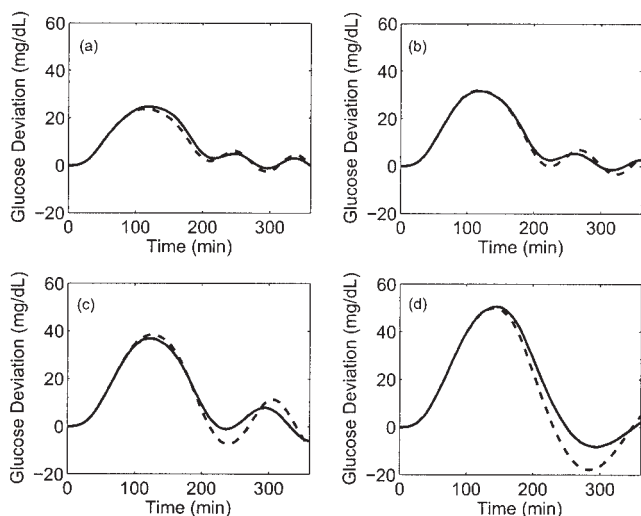


**Figure 7. System outputs given the disturbance in Figure 5 under MPC (dashed) and NMPC (solid) control for various values of  $\Gamma_{uc}$ .**

(a)  $\Gamma_{uc} = 0.001$ , (b)  $\Gamma_{uc} = 0.01$ , (c)  $\Gamma_{uc} = 0.1$ , (d)  $\Gamma_{uc} = 1.0$ .  $p = 70$ ,  $c = 5$ ,  $\Gamma_{yc} = \alpha_c = 1$ .

terms of peak glucose magnitude. The optimal PD response has a significantly reduced peak but yields glucose values that do not approach zero within the trial time length. The MPC and NMPC algorithms both perform very aggressively but with a numerical performance improvement for the NMPC algorithm over MPC. These results agree with the control-relevant nonlinearity assessment indicating low control-relevant nonlinearity because there is not a significant benefit in using a nonlinear model in the algorithm. Although there is a significant benefit in proceeding from the PD to MPC algorithms, this is likely

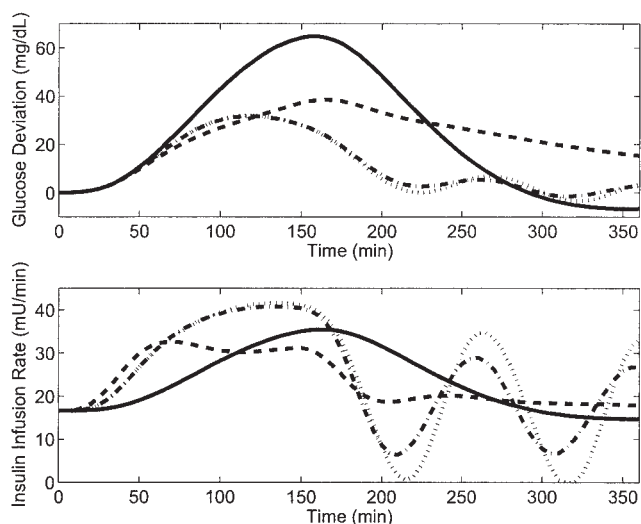


**Figure 8. Closed-loop outputs (top) and inputs (bottom) for trials in which the performance objective (Eq. 18) is optimized with  $\alpha = 1$ ,  $\Gamma_y = 1$ , and  $\Gamma_u = 1$ .**

Solid = P-only; dashed = PD; dotted = MPC; dash-dotted = NMPC (tunings found in Table 2).

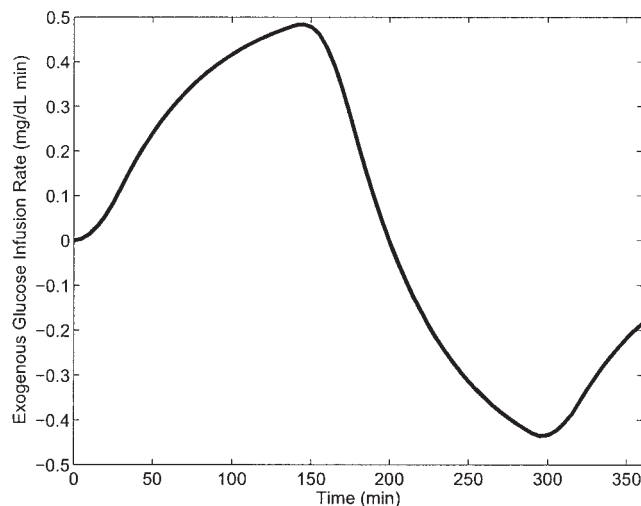


**Figure 9. Exogenous glucose infusion trajectory  $[P(t)]$  in Eq. 16] used to assess controller performance given the asymmetric performance objective.**

attributable more to the nature of the dynamics and the disturbance than to any nonlinear effects.

The second set of trials are performed with the performance objective including the following weights:  $\alpha = 20$ ,  $\Gamma_y = 1$ , and  $\Gamma_u = 1$ . Based on the  $\alpha$ -value, this trial represents a highly asymmetric objective in which negative deviations are penalized 20 times as much as positive deviations in glucose. Recall that the control-relevant nonlinearity for this situation, as shown in Figure 4, is 0.90.

For this trial, two different version of the MPC and NMPC algorithms are investigated. For both types of MPC, one algorithm contains a symmetric performance objective (Eq. 24 with  $\alpha_c = 1$ ) and the other has an asymmetric performance objective (Eq. 24 with  $\alpha_c = 20$ ). This brings the total number of controllers considered to six:

- (1) P-only
- (2) PD
- (3) MPC with a quadratic performance objective ( $\alpha_c = 1$ )
- (4) MPC with an asymmetric performance objective ( $\alpha_c = 20$ )
- (5) NMPC with a quadratic performance objective ( $\alpha_c = 1$ )
- (6) NMPC with an asymmetric performance objective ( $\alpha_c = 20$ )

Controllers 1–3 are linear algorithms, whereas controllers 4–6 are nonlinear algorithms. Note that, although controller 4 includes a linear system model, the inclusion of an asymmetric objective function results in a nonlinear algorithm.

Because the meal disturbance in Figure 5 does not yield significantly negative glucose deviations, there will be little difference in tuning the controllers to optimize an asymmetric objective function compared to the symmetric objective function. Therefore, the less realistic disturbance shown in Figure 9 is considered for the second trial to provoke negative glucose deviations. This type of disturbance may be thought of as a meal followed by exercise, for example. Note that the use of this type of disturbance assumes that the dynamics of the glucose absorption and removal processes are the same.

The controller tunings and performance objective results for this trial are found in Table 3 with the minimum ( $G_{\min}$ ) and maximum ( $G_{\max}$ ) value of glucose reached along the corre-



**Table 3. Controller Tunings and Performance Metrics for Trials with  $\alpha = 20$ ,  $\Gamma_y = 1$ , and  $\Gamma_u = 1$  in Eq. (18)**

Controller	Tunings	Objective Value	$G_{\min}$ (mg/dL)	$G_{\max}$ (mg/dL)
P-only	$K_c = -0.04$	$1.17 \times 10^5$	-9.87	52.20
PD	$K_c = -0.02$ , $K_d = 186$	$1.16 \times 10^5$	-3.45	30.66
MPC	$p = 30$ , $c = 5$ , $\Gamma_{uc} = 0.00015$ , $\Gamma_{yc} = 1.0$ , $\alpha_c = 1$	$1.66 \times 10^5$	-8.99	8.78
MPC	$p = 30$ , $c = 5$ , $\Gamma_{uc} = 0.00015$ , $\Gamma_{yc} = 1.0$ , $\alpha_c = 20$	$1.04 \times 10^5$	-6.45	9.06
NMPC	$p = 30$ , $c = 5$ , $\Gamma_{uc} = 0.00015$ , $\Gamma_{yc} = 1.0$ , $\alpha_c = 1$	$1.63 \times 10^5$	-8.90	8.85
NMPC	$p = 30$ , $c = 5$ , $\Gamma_{uc} = 0.00015$ , $\Gamma_{yc} = 1.0$ , $\alpha_c = 20$	$1.01 \times 10^5$	-6.44	9.09

sponding output trajectories also reported. Figure 10 includes the trajectories for the P-only, PD, and the MPC algorithms that include  $\alpha_c = 1$ . The results in Figure 10 and Table 3 show that the P-only and PD algorithms optimize the desired performance by allowing for an undesirably large (given the disturbance magnitude) positive deviation in glucose to avoid the more costly negative deviations. Note the substantially large derivative gain necessary to optimize PD performance. Although the MPC algorithms actually show a decreased level of performance in terms of the performance objective, their trajectories are considerably more desirable in terms of avoiding large positive deviations with an acceptable increase in  $G_{\min}$  magnitude, although this was not the objective of the tuning procedure.

Figure 11 provides a comparison of the four MPC algorithms. Figure 11 shows that there is a visual difference between the output trajectories for the MPC controllers with and without the included asymmetric performance objective only at the end of the trial length when the negative glucose deviations are most severe. Table 3 shows that the asymmetric algorithms provide a significant benefit over their symmetric counterparts in both objective function value and  $G_{\min}$  without a significant increase in  $G_{\max}$ . A key difference in the results, as seen in Figure 11, is that the algorithms that include the asymmetric objective reach the lower constraint on insulin infusion rate. Note that no explicit constraint handling capabilities are in-

cluded in the MPC algorithms. Inputs below  $-16.7$  mU/min are clipped by the controllers and set to  $-16.7$  mU/min.

As an experiment to isolate any performance loss arising from clipping of the controller outputs to handle constraints, soft constraints are added to the asymmetric MPC algorithms. To do so, the MPC performance objective (Eq. 24) is augmented with the following term

$$\dots + \Gamma_c \min[u(k+i-1) + 16.7, 0]^2 \quad (27)$$

where  $\Gamma_c$  was taken to be  $1 \times 10^4$  to provide a substantial penalty on insulin rates below  $-16.7$  mU/min. Using the same tunings as in Table 3 for MPC and NMPC (with  $\alpha_c = 20$ ), the results in Table 4 are obtained. The results show performance that is slightly worse than that of the asymmetric algorithms with clipping likely resulting from the sluggishness introduced by penalizing deviations below the constraint at all times, including in the prediction of future moves. In summary, it appears that clipping of controller outputs does not adversely affect performance.

To summarize the trial with the asymmetric performance objective, the results indicate an increased level of control-relevant nonlinearity for this case as predicted by the theoretical control-relevant nonlinearity assessment. For this example, there is a significant benefit in using nonlinear control. Specif-

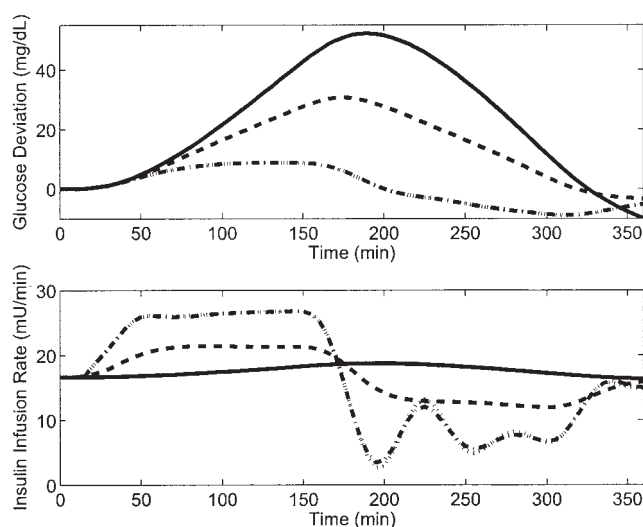


**Figure 10. Closed-loop outputs (top) and inputs (bottom) for trials in which performance objective (Eq. 18) is optimized with  $\alpha = 20$ ,  $\Gamma_y = 1$ , and  $\Gamma_u = 1$ .**

Solid = P-only; dashed = PD; dotted = MPC ( $\alpha_c = 1$ ); dash-dotted = NMPC ( $\alpha_c = 1$ ) (tuning values in Table 3).

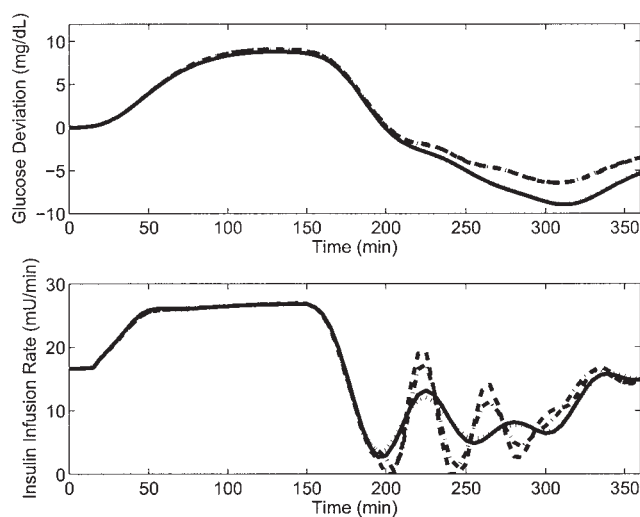


**Figure 11. Closed-loop outputs (top) and inputs (bottom) for MPC trials in which the performance objective (Eq. 18) is optimized with  $\alpha = 20$ ,  $\Gamma_y = 1$ , and  $\Gamma_u = 1$ .**

Solid = MPC with  $\alpha_c = 1$ ; dashed = MPC with  $\alpha_c = 20$ ; dotted = NMPC with  $\alpha_c = 1$ ; and dash-dotted = NMPC with  $\alpha_c = 20$  (tuning values in Table 3).

**Table 4 Performance Results for the Asymmetric MPC and NMPC Algorithms with Soft Constraints on Controller Output**

Controller	Tunings	Objective Value	$G_{\min}$ (mg/dL)	$G_{\max}$ (mg/dL)
MPC	$p = 30, c = 5, \Gamma_{uc} = 0.00015, \Gamma_{yc} = 1.0, \alpha_c = 20$	$1.24 \times 10^5$	-6.76	9.79
NMPC	$p = 30, c = 5, \Gamma_{uc} = 0.00015, \Gamma_{yc} = 1.0, \alpha_c = 20$	$1.24 \times 10^5$	-6.94	10.52

ically, a linear MPC algorithm with an asymmetric objective function appears to be the highest complexity algorithm necessary. Although the simple P-only and PD controllers perform well in terms of the objective function value, this performance comes at the cost of large positive deviations in glucose. The MPC and NMPC algorithms with asymmetric performance objectives are able to reduce the performance objective values and  $G_{\min}$  magnitude without a significant increase in  $G_{\max}$ . This trial again shows the limited benefit in including a nonlinear model in the control algorithm, given that the MPC algorithms with linear and nonlinear models perform similarly. As predicted by the theoretical assessment, the primary influence on the control-relevant nonlinearity comes from the performance objective and not the system model.

## Conclusions

The results of this study suggest that linear model-based control is the highest level of complexity necessary for regulation of glucose. Although a benefit was shown in incorporating an asymmetric objective function in the linear MPC algorithm, it appears that linear MPC with a quadratic objective function would generally be sufficient provided that it is tuned appropriately. No significant benefit was found in incorporating a nonlinear model in a control algorithm. Even though there would be no harm in use of a well-identified nonlinear model in a glucose controller, there is no reason to expect a significant increase in performance to justify the extra effort required to implement and maintain a nonlinear model-based technique. The results of this work also discourage use of low-complexity (such as PD) control if high levels of performance are desired.

In this study, the theoretical and performance-based control-relevant nonlinearity results agree in the sense that the greatest nonlinear influence comes from the performance objective and not the process model. As the performance objective becomes more nonlinear, the resulting control problem becomes more challenging, but remains amenable to linear techniques. In general, characterization of the OCS was shown to be an excellent metric for predicting and analyzing these types of effects.

Although the range of glucose values investigated was not varied in this work's analysis, a system's operating region tends to have a significant effect on its control-relevant nonlinearity. Therefore, if larger glucose excursions are considered, it is likely that the degree of control-relevant nonlinearity will increase. The glucose range considered in this work was carefully selected to represent typical excursions.

Models for diabetic systems are, by nature, imprecise. Therefore, another factor that discourages use of PID-type algorithms is the issue of robustness. The extra robustness properties inherently afforded by an MPC algorithm—stemming from its ability to correct predictions based on current measurements—makes it the best choice, given the analysis performed here. Future study should consider more detailed system models to verify these findings. Additional effects, such

as the effects of system noise on controller performance, could also be taken into account in terms of the analysis procedures presented here.

## Literature Cited

1. The Diabetes Control and Complications Trial Research Group. The effect of intensive treatment of diabetes on the development and progression of long-term complications in insulin-dependent diabetes-mellitus. *N. Engl. J. Med.* 1993;329:977-986.
2. Wolpert HA. A clinician's perspective on some challenges in "closing the loop." *Diabetes Technol. Ther.* 2003;5:843-846.
3. MiniMed® CGMS®. Information available at: [http://www.minimed.com/patientfam/pf\\_products\\_cgms\\_ov\\_completepic.shtml](http://www.minimed.com/patientfam/pf_products_cgms_ov_completepic.shtml).
4. Glucowatch®. Information available at: <http://www.glucowatch.com>.
5. Disetronic. Information available at: <http://www.disetronic-usa.com/insulin-pumps.htm>.
6. MiniMed® Paradigm® Insulin Pump. Information available at: [http://www.minimed.com/patientfam/pf\\_ipt\\_paradigm\\_insulin\\_pump.shtml](http://www.minimed.com/patientfam/pf_ipt_paradigm_insulin_pump.shtml).
7. Lam Z-H, Hwang K-S, Lee J-Y, Chase JG, Wake GC. Active insulin infusion using optimal and derivative-weighted control. *Med. Eng. Phys.* 2002;24:663-672.
8. Panteleon AE, Loutseiko M, Steil GM, Rebrin K. A novel approach for closed loop control of meal induced carbohydrate intake. *Proc. of Third Annual Diabetes Technology Meeting*, San Francisco, CA; November 2003.
9. Parker RS, Doyle FJ III, Peppas NA. A model-based algorithm for blood glucose control in type I diabetic patients. *IEEE Trans. Biomed. Eng.* 1999;46:148-157.
10. ADICOL Project. Information available at: [http://www.adicol.org/project/posters/year\\_2002/dtm\\_2002\\_dms.pdf](http://www.adicol.org/project/posters/year_2002/dtm_2002_dms.pdf).
11. Ollerton RL. Application of optimal control theory to diabetes mellitus. *Int. J. Control.* 1989;50:2503-2522.
12. Fisher MEA. Semiclosed-loop algorithm for the control of blood glucose levels in diabetics. *IEEE Trans. Biomed. Eng.* 1991;38:57-61.
13. Parker RS, Gatzke EP, Doyle FJ III. Advanced Model Predictive Control (MPC) for Type I Diabetic Patient Blood Glucose Control. In: *Proceedings of the American Control Conference*. Chicago, IL; 2000: 3483-3487.
14. Hernjak N, Doyle FJ III. Correlation of process nonlinearity with closed-loop disturbance rejection. *Ind. Eng. Chem. Res.* 2003;42:4611-4619.
15. Desoer CA, Wang Y. Foundations of feedback theory for nonlinear systems. *IEEE Trans. Circ. Syst.* 1980;CAS-27:104-123.
16. Haber R. Nonlinearity test for dynamic processes. *Proc. of the IFAC Identification and System Parameter Estimation Symposium*. Elmsford, NY: Pergamon Press; 1985:409-414.
17. Ogunnaike BA, Pearson RK, Doyle FJ III. Chemical process characterization: With applications in the rational selection of control strategies. *Proc. of the European Control Conference*. Groningen, The Netherlands; 1993:1067-1071.
18. Guay M, McLellan P, Bacon D. Measurement of nonlinearity in chemical process control systems: The steady-state map. *Can. J. Chem. Eng.* 1995;73:868-882.
19. Nikolaou M, Hanagandi V. Nonlinear quantification and its application to nonlinear system identification. *Chem. Eng. Commun.* 1998;166:1-33.
20. Hahn J, Edgar TF. A gramian-based approach to nonlinearity quantification and model classification. *Ind. Eng. Chem. Res.* 2001;40:5724-5731.
21. Allgöwer F. Definition and computation of a nonlinearity measure. *Proc. of the 3rd IFAC Nonlinear Control Systems Design Symposium*. Elmsford, NY: Pergamon Press; 1995:279-284.
22. Helbig A, Marquardt W, Allgöwer F. Nonlinearity measures: Definition, computation and applications. *J. Process Control.* 2000;10:113-123.

23. Stack AJ, Doyle FJ III. The optimal control structure approach to measuring control-relevant nonlinearity. *Comput. Chem. Eng.* 1997; 21:998-1009.
24. Sorensen JT. *A Physiologic Model of Glucose Metabolism in Man and Its Use to Design and Assess Improved Insulin Therapies for Diabetes*. PhD Thesis. Dept. of Chemical Engineering, MIT, Cambridge, MA; 1985.
25. Bergman RN, Phillips LS, Cobelli C. Physiologic evaluation of factors controlling glucose tolerance in man. *J. Clin. Invest.* 1981;68:1456-1467.
26. Furler SM, Kraegen EW, Smallwood RH, Chisolm DJ. Blood glucose control by intermittent loop closure in the basal mode: Computer simulation studies with a diabetic model. *Diabetes Care.* 1985;8:553-561.
27. Prett DM, Garcia CE. *Fundamental Process Control*. Boston, MA: Butterworth-Heinemann; 1998.
28. Allgöwer F, Badgwell TA, Qin JS, Rawlings JB, Wright SJ. Nonlinear predictive control and moving horizon estimation—An introductory overview. *Advances in Control—Highlights of ECC '99*. London: Springer-Verlag; 1999:391-449.
29. Lehmann ED, Deutsch T. A physiological model of glucose-insulin interaction in type I diabetes mellitus. *J. Biomed. Eng.* 1992;14:235-242.

*Manuscript received Jan. 30, 2004, and revision received Jun. 9, 2004.*